

Abstract. Tropospheric aerosols have a significant influence on climate and have been recognised by the Intergovernmental Panel on Climate Change as the biggest source of uncertainty in understanding future climate, yet the factors controlling their spatial distribution remain unclear. New observations from the UK ATSR instruments and the MODIS instrument (on NASA's Terra and Aqua satellites) provide global estimates of aerosol optical thickness and particle effective radius. This is significant progress on previously available measurements, but leaves open questions about aerosol sources, sinks, microphysical properties and the aerosol vertical distribution. A one-dimensional dust lifting model, using meteorological fields from ECMWF analyses, is used to compare predicted dust loading with observations. The model will be used to investigate the sensitivity of the predicted aerosol profiles to variations in model parameters.

Introduction and Method

Large scale dust storms have been observed coming off the Sahara desert [Slingo *et al.*, 2006] by satellite instruments such as SEVIRI, but these instruments cannot accurately assess the spatial distribution of aerosol particle sizes. The aim of the current work is to predict the transport of desert aerosol using meteorological and soil data. Further work will involve assimilation to compare with observations, and extension to three dimensions.

The one-dimensional model is driven by meteorological data from the European Centre for Medium-range Weather Forecasting (ECMWF) operational data set (u , v , w , T , on 91 hybrid levels at a resolution of 1.125°) and by soil data from the International Satellite Land Surface Climatology Project (ISLSCP), which provides an estimate of the distribution of particle sizes, at a resolution of 1° .

Implicit within the model is the role that *saltation* and *sand-blasting* have in mobilising and emitting dust particles from the surface: saltation is a transport mechanism in which sand particles are ejected and thrown forward several metres in a parabolic path, and when they strike the surface again they eject (sand-blast) more particles. The emission flux is dependent on the horizontal saltation flux, and is described by Ginoux *et al.* (2001) using the semi-empirical formula:

$$F = Csu^2(u - u_t) \quad (1)$$

C is a factor equal to $1 \mu\text{g s}^2\text{m}^{-5}$, s is the source fraction term which determines the fraction of a particular size class within the soil, u is the horizontal wind speed at 10 m altitude, and $u_t(r)$ is the threshold wind velocity.

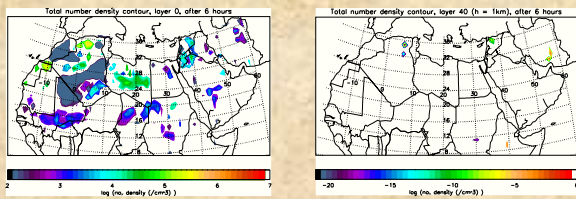


Figure 5: Results from the 1-D model run at every location within the Sahara region, after 6 hours. Layer 0 (left) is the saltation (surface) layer, the areas of greatest activity are northern Algeria and the Western Sahara. In layer 40 ($h = 1 \text{ km}$) the number density has diminished dramatically, and the areas of greatest activity have shifted, eg. to Iran.

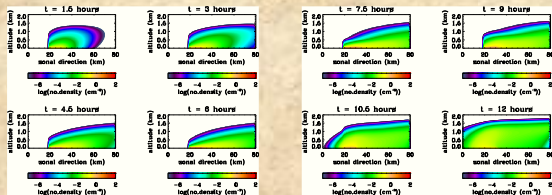


Figure 6: Preliminary results from the 2D model, from 1/2/2006, at 38.25°E , 28.125°N . A strip of land 12 km long is a dust source.

References

- Ginoux P *et al.* (2001). Sources and distributions of dust aerosols simulated with the GOCART model, *J. Geophys. Res.*, Vol. 106, No. D17
Slingo A *et al.* (2006). Observations of the impact of a major Saharan dust storm on the atmospheric radiation balance, *Geophys. Res. Lett.*, Vol. 33

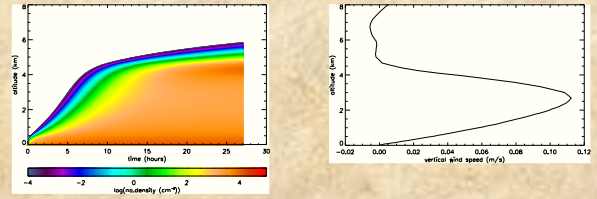


Figure 2: Model simulation of the evolution of particle number density over time, in the steady state. Conditions are taken from 12.00 on 16/5/2006, at 38.25°E , 28.125°N , in the north-west of Saudi Arabia. The vertical wind velocity profile is on the right.

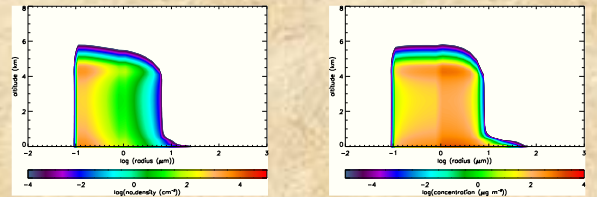


Figure 3: Distribution of number density (left) and concentration (right) with particle radius. Note how the peak in concentration occurs at $r = 1.0 \mu\text{m}$, while the peak in number density occurs at $r = 0.13 \mu\text{m}$: this is due to larger particles carrying more mass. Note also that the plume that develops at 4500 m dips slightly for larger particles ($> 1 \mu\text{m}$).

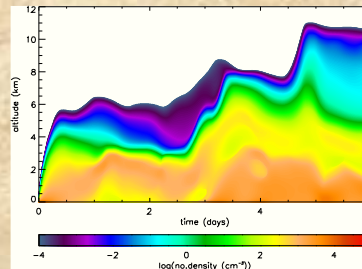
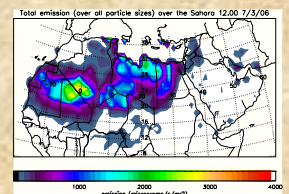


Figure 4: Results from a model taking into account varying meteorological conditions, from the same location and time as above. The wind fields are interpolated to every 20 minutes.

Figure 1: Plot of the total mass flux of particles being emitted from the surface of the Sahara at noon on 7/3/2006.



Due to particle falling velocities (which are proportional to particle radius squared), the larger particles ($> 10 \mu\text{m}$) quickly drop back to the surface. Finer particles (with radii typically less than $1-2 \mu\text{m}$) can be transported to higher altitudes (up to 8 km or so) through the influence of vertical wind velocities and turbulent diffusion.

The method used to calculate the evolution of the concentration in each layer of the atmosphere is a finite difference method. Between layers 1 and 2, the flux is dependent on the concentration in each layer, χ_1 and χ_2 , the vertical wind velocity at that altitude, w , the particle fall velocity for that size, w_{fall} , the thickness of the layer, δz , and the vertical turbulent diffusion coefficient, K_{zz} . An 'upstream' approximation is used.

$$F_{1,2} = (w - w_{\text{fall}})\chi_1 - (K_{zz}/\delta z)(\chi_2 - \chi_1) \quad (2)$$

If $w > w_{\text{fall}}$ then $\chi = \chi_1$, and if $w < w_{\text{fall}}$ then $\chi = \chi_2$. The tendency, $\delta\chi_2/\delta t$ in layer 2 is given by:

$$\delta\chi_2/\delta t = (F_{2,3} - F_{1,2})/\delta z \quad (3)$$

This is multiplied by the time step dt to find the concentration χ_2 .

The 2D model adds the x-direction (zonal) to this scheme, with a box width δx and a horizontal wind speed u . The 2D model can be extended to 3D.